# Efficient Hybrid onboard & offboard charging for optimizing EV Performance

Diksha Khare[1], Dr.Nitin Dhote[2], Prof.Rajendra Bhombe[3][
[1]*Guru Nanak Institute of Engineering & Technology, Nagpur*
[2]*St.Vincent Palloti College of Engineering, Nagpur*
[3]*Guru Nanak Institute of Engineering & Technology, Nagpur*

***Abstract*—In this study, we present a multilayer DC-DC converter design that was inspired by biology for the purpose of speeding the charging of plug-in hybrid vehicles and electric vehicles (EVs and PHEVs). The unregulated power from the front-end ac-dc converter is sent to the dc-dc converter's specified bioinspired design, where it is then utilised by the EV propulsion battery. A bio-inspired, multilayer, isolated dc-dc converter as a technique to allow quick battery charging for electric vehicle batteries is suggested. This converter would be isolated and would have bio-inspired layers.**

***Index Terms*— Multilayer DC-DC converter, bioinspired design, plug-in hybrid vehicles**

## I. INTRODUCTION

There has been a notable increase in the number of individuals driving electric cars [1,] which may be attributed to the growing concerns over the effect that emissions from automobiles have on the environment. (EVs). It is anticipated that electric cars would account for thirty percent of the market by the year 2030 [2]. The ever-increasing market share of electric vehicles calls for persistent enhancements to the infrastructure used for charging such vehicles. Direct current fast charging (DCFC) stations, vehicle on-board chargers (OBCs), and electric vehicle supply equipment make up the vast bulk of the existing charging infrastructure (EVSE). In-vehicle chargers are by far the most prevalent kind of charging source, and they can be found in the great majority of vehicles [3]. They are also the most convenient type of charging source.

## II. PROPOSED METHODOLOGY

Figure 1 provides a representation of the multilevel dc-dc architecture in the form of a schematic diagram. The output of the front-end ac-dc converter is wired to a full-bridge network, which consists of MOSFETs Q1 and Q4, and is linked to the network. The DC bus is connected to this output right here. On the battery side of the circuit, in addition to a number of switches and diodes, there are also two voltage doubler rectifiers, which are designated by the numerals D1-D2 and D3-D4, respectively (Q5, D5, and D6). These components are used to shift the outputs of the voltage doubler into series and parallel, which enables a wide range of voltage levels to be given. The needed resonance frequency served as the criterion for determining which of the four capacitors, C1 through C4, would be used to construct the voltage doubler. These capacitors are identical in every respect. By using a high-frequency transformer that consists of three windings, both the direct current bus and the battery are maintained galvanically separated from one another (HFT). The voltage that is produced as a consequence of the phase-shifted action of the legs of the full-bridge circuit represents a square wave. This phenomenon may be seen. Because of the adjustment made to the intermediate switch, the rectified outputs of the voltage doubler are subjected to synthesis, which results in the production of a multilayer voltage that is produced at a frequency that is twice as high as the switching frequency. This voltage is produced at a frequency that is twice as high as the switching frequency (Q5).

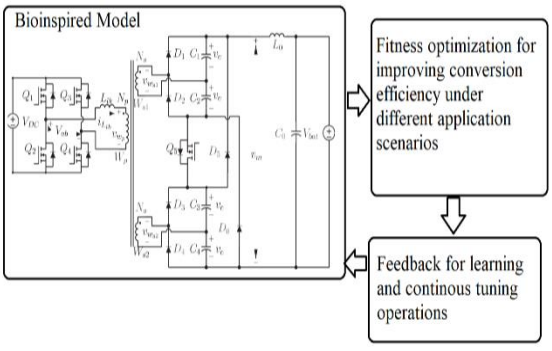


Figure 1. Design of the proposed model for efficiency optimizations.

It is assumed that there are no parasitic series resistances, that all of the capacitors C1–C4 have the same value, and that the voltage and current induced on the two secondary windings Ws1 and Ws2 are the same regardless of the application that is being considered. In addition, it is assumed that there are no differences in the values of the capacitors. Every one of these factors is taken into consideration. Within the confines of a single switching cycle, the functionality of the converter may be partitioned into a total of 10 distinct modes, as can be seen in the illustration. Due to the fact that the functioning of the converter is symmetrical around a half-wave, just one half of the processes that occur during the switching cycle will be addressed in this article. The comparable circuits that are used by the converter in each of its many modes of operation are seen in the figure sets.

Mode 1 encompasses t0, t, and t1 in its definition (t0, t, and t1) After the conditions for zero voltage switching (ZVS) have been met, the switch Q1 will become active very early on in this mode. As a consequence of the charging and discharging of the output capacitor, the gate signal for Q2 was blocked prior to the switch being made to this mode, and during that time, an antiparallel diode was connected to Q1 (controlled by the cos values of switches Q2 and Q1, respectively). Because of this, the total conversion efficiency will be boosted over a broad spectrum of application circumstances as a direct consequence of the use of bioinspired optimization with continuous feedbacks, which will improve these model parameter sets.

On Board Charging Process

The BLIL PFC boost converter [20–23] utilizes the following components to carry out this process: four inductors (L1, L2, L3, and L4), four power MOSFETs (Q1 to Q4), four diodes (D1 to D4), and an intermediate DC link capacitor (C01). As the name implies, the diode bridge rectifier has been eliminated from the circuit. The four channel interleaving boost converter exhibited much less input current ripple than the standard interleaved boost converter. Input current is equal to the sum of the currents flowing via inductors L1/L2 and L3/L4. As a result of the fact that the ripple currents in the inductors [L1/L2 and L3/L4] are no longer in phase with one another [24], the ripple of the input current has been substantially reduced. Interleaving reduces electromagnetic interference (EMI) in a circuit, along with current stress on the devices and ripple in the output capacitor [25]. For the development of the BLIL boost converter, the PFC control algorithm is used. This enhances the power factor and power quality of the input current in accordance with IEC standard 61000-2-3. Moreover, the voltage across the load may be adjusted to the desired level. There are several strategies for forming the PFC [26, 27], including the boundary conduction mode (BCM), the continuous conduction mode (CCM), and the discontinuous conduction mode (DCM) (DCM). In boost PFC converters, the management of the average current mode, often known as ACM, is commonly regarded as one of the most effective means of achieving high power factor and little distortion. + This solution has the drawback of requiring the detection of input current, input voltage, output voltage, and a multiplier circuit, which makes the circuit more complex. Whenever there is an interruption in the line voltage, the ACM control mechanism will make the necessary adjustments. This will result in an increase in the output voltage's resistance to supply line variations. The system requires a considerable number of switching cycles to attain a steady state since the outer voltage loop reacts slowly to transients. However, these drawbacks may be eliminated by using a nonlinear control approach. Resettable integrator control is used to govern the CCM mode-operating BLIL boost converter that is the subject of this study. The resettable integrator (RI) approach is presented for use with converters that operate at a constant frequency [28–30]. +is control does not require an input voltage sensor, multipliers, or an input current error compensator. The opposite of average current mode control. This control strategy enables for the reduction of harmonics while still monitoring transients, which is a considerable benefit. In this stage, the output signal is blended until it is nearly equivalent to the reference signal. Both the frequency of the input signal, x(t), and the frequency of the reference signal, Vr(t), may be regarded as constants even though the switching frequency of the converter, f0, is much greater than both of these frequencies. The output variable's settings should be y(t) for real-time scenarios.

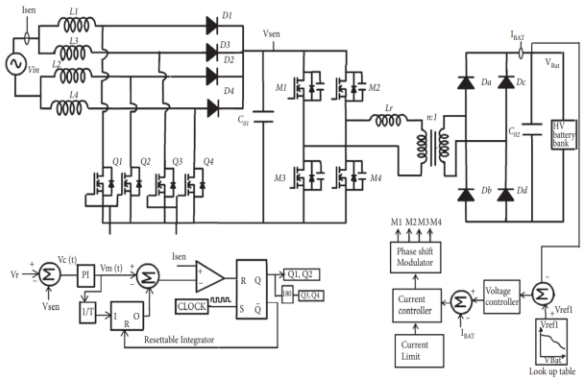


Figure 2. The on-board charging processes

Off Board Charging Process

Figure 3 depicts the converter's proposed architecture. The suggested construction consists of five elements in total, as shown in the following figure: two power electronic switches, two inductors, three capacitors, and three diodes. The suggested architecture is switched using the PWM technique, and the switches used to turn them on and off complement one another. The suggested architecture has a sizable voltage gain and does not need the use of a high-frequency transformer; nevertheless, its main disadvantage is that it requires challenging switching conditions. The energy storage element feature, which includes capacitors and inductors among other parts, is used to achieve the advised converter voltage gain. The following conditions are presumed to be true in order to streamline the analysis: (a) the converter is operating in steady state, which means that the output voltage Vo is constant; (b) the capacitors are sufficiently large for their voltage to remain constant throughout each switching period; (c) all switches and diodes are perfect; (d) equivalent series resistance (ESR) ESR is ignored; and (e) the isolation of the system is completed before the converters.

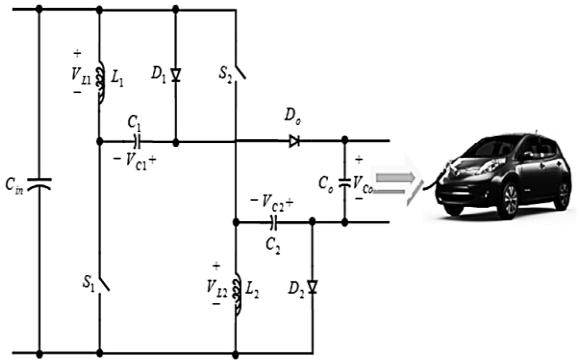


Figure 3. Design of the off-board charging process

## III. CONCLUSION

A bio-inspired, multilayer, isolated dc-dc converter as a technique to allow quick battery charging for electric vehicle batteries is suggested. This converter would be isolated and would have bio-inspired layers. Because of the design of the voltage doubler and the ability to reposition the voltage doubler units in series or parallel by adjusting an intermediary device that produces multilayer voltage, the proposed converter may have a high voltage gain and a wide voltage range. These features are made possible by the construction of the voltage doubler. The better power conversion efficiency that has been noticed as a consequence of its employment may be attributed to the recommended modulation approach, which enables full-bridge devices to engage in soft switching. This has been made possible as a result of the utilization of the technology.

## REFERENCE

[1] R. Yang, R. Xiong and W. Shen, "On-board diagnosis of soft short circuit fault in lithium-ion battery packs for electric vehicles using an extended Kalman filter," in CSEE Journal of Power and Energy Systems, vol. 8, no. 1, pp. 258-270, Jan. 2022, doi: 10.17775/CSEEJPES.2020.03260.

[2] X. Piao, X. Wang and K. Han, "Hierarchical Model Predictive Control for Optimization of Vehicle Speed and Battery Thermal Using Vehicle Connectivity," in IEEE Access, vol. 9, pp. 141378-141388, 2021, doi: 10.1109/ACCESS.2021.3120406.

[3] W. D. Connor, Y. Wang, A. A. Malikopoulos, S. G. Advani and A. K. Prasad, "Impact of Connectivity on Energy Consumption and Battery Life for Electric Vehicles," in IEEE Transactions on Intelligent Vehicles, vol. 6, no. 1, pp. 14-23, March 2021, doi: 10.1109/TIV.2020.3032642.

[4] T. A. Lehtola and A. Zahedi, "Electric Vehicle Battery Cell Cycle Aging in Vehicle to Grid Operations: A Review," in IEEE Journal of Emerging and Selected Topics in Power Electronics, vol. 9, no. 1, pp. 423-437, Feb. 2021, doi: 10.1109/JESTPE.2019.2959276.

[5] W. Kim, P. -Y. Lee, J. Kim and K. -S. Kim, "A Robust State of Charge Estimation Approach

Based on Nonlinear Battery Cell Model for Lithium-Ion Batteries in Electric Vehicles," in IEEE Transactions on Vehicular Technology, vol. 70, no. 6, pp. 5638-5647, June 2021, doi: 10.1109/TVT.2021.3079934.

[6] D. Li, Z. Zhang, P. Liu, Z. Wang and L. Zhang, "Battery Fault Diagnosis for Electric Vehicles Based on Voltage Abnormality by Combining the Long Short-Term Memory Neural Network and the Equivalent Circuit Model," in IEEE Transactions on Power Electronics, vol. 36, no. 2, pp. 1303-1315, Feb. 2021, doi: 10.1109/TPEL.2020.3008194.

[7] J. Hong et al., "Thermal Runaway Prognosis of Battery Systems Using the Modified Multiscale Entropy in Real-World Electric Vehicles," in IEEE Transactions on Transportation Electrification, vol. 7, no. 4, pp. 2269-2278, Dec. 2021, doi: 10.1109/TTE.2021.3079114.

[8] Q. Wang, Z. Wang, L. Zhang, P. Liu and Z. Zhang, "A Novel Consistency Evaluation Method for Series-Connected Battery Systems Based on Real-World Operation Data," in IEEE Transactions on Transportation Electrification, vol. 7, no. 2, pp. 437-451, June 2021, doi: 10.1109/TTE.2020.3018143.

[9] H. M. Khalid, F. Flitti, S. M. Muyeen, M. S. Elmoursi, T. O. Sweidan and X. Yu, "Parameter Estimation of Vehicle Batteries in V2G Systems: An Exogenous Function-Based Approach," in IEEE Transactions on Industrial Electronics, vol. 69, no. 9, pp. 9535-9546, Sept. 2022, doi: 10.1109/TIE.2021.3112980.

[10] L. Zhou, Y. Zhao, D. Li and Z. Wang, "State-of-Health Estimation for LiFePO4 Battery System on Real-World Electric Vehicles Considering Aging Stage," in IEEE Transactions on Transportation Electrification, vol. 8, no. 2, pp. 1724-1733, June 2022, doi: 10.1109/TTE.2021.3129497.

[11] H. Wu, "A Survey of Battery Swapping Stations for Electric Vehicles: Operation Modes and Decision Scenarios," in IEEE Transactions on Intelligent Transportation Systems, vol. 23, no. 8, pp. 10163-10185, Aug. 2022, doi: 10.1109/TITS.2021.3125861.

[12] S. Li, P. Zhao, C. Gu, J. Li, S. Cheng and M. Xu, "Online Battery Protective Energy Management for Energy-Transportation Nexus," in IEEE Transactions on Industrial Informatics, vol. 18, no. 11, pp. 8203-8212, Nov. 2022, doi: 10.1109/TII.2022.3163778.

[13] Q. Shi, Z. He, Y. Wei, M. Wang, X. Zheng and L. He, "Single Pedal Control of Battery Electric Vehicle by Pedal Torque Demand With Dynamic Zero Position," in IEEE Transactions on Intelligent Transportation Systems, vol. 23, no. 11, pp. 21608-21619, Nov. 2022, doi: 10.1109/TITS.2022.3181042.

[14] L. Jiang et al., "Optimal Charging Strategy With Complementary Pulse Current Control of Lithium-Ion Battery for Electric Vehicles," in IEEE Transactions on Transportation Electrification, vol. 8, no. 1, pp. 62-71, March 2022, doi: 10.1109/TTE.2021.3097135.

[15] D. Li et al., "Battery Thermal Runaway Fault Prognosis in Electric Vehicles Based on Abnormal Heat Generation and Deep Learning Algorithms," in IEEE Transactions on Power Electronics, vol. 37, no. 7, pp. 8513-8525, July 2022, doi: 10.1109/TPEL.2022.3150026.

[16] D. Cui, Z. Wang, Z. Zhang, P. Liu, S. Wang and D. G. Dorrell, "Driving Event Recognition of Battery Electric Taxi Based on Big Data Analysis," in IEEE Transactions on Intelligent Transportation Systems, vol. 23, no. 7, pp. 9200-9209, July 2022, doi: 10.1109/TITS.2021.3092756.

[17] T. M. N. Bui, M. Sheikh, T. Q. Dinh, A. Gupta, D. W. Widanalage and J. Marco, "A Study of Reduced Battery Degradation Through State-of-Charge Pre-Conditioning for Vehicle-to-Grid Operations," in IEEE Access, vol. 9, pp. 155871-155896, 2021, doi: 10.1109/ACCESS.2021.3128774.

[18] Z. He, Q. Shi, Y. Wei, J. Zheng, B. Gao and L. He, "A Torque Demand Model Predictive Control Approach for Driving Energy Optimization of Battery Electric Vehicle," in IEEE Transactions on Vehicular Technology, vol. 70, no. 4, pp. 3232-3242, April 2021, doi: 10.1109/TVT.2021.3066405.

[19] J. Wu, X. Cui, H. Zhang and M. Lin, "Health Prognosis With Optimized Feature Selection for Lithium-Ion Battery in Electric Vehicle Applications," in IEEE Transactions on Power Electronics, vol. 36, no. 11, pp. 12646-12655, Nov. 2021, doi: 10.1109/TPEL.2021.3075558.

[20] K. Shipra, R. Maurya and S. N. Sharma, "Brayton-moser passivity based controller for electric vehicle battery charger," in CPSS Transactions on Power Electronics and Applications, vol. 6, no. 1, pp. 40-51, March 2021, doi: 10.24295/CPSSTPEA.2021.00004.

[21] N. Gan, Z. Sun, Z. Zhang, S. Xu, P. Liu and Z. Qin, "Data-Driven Fault Diagnosis of Lithium-Ion Battery Overdischarge in Electric Vehicles," in IEEE Transactions on Power Electronics, vol. 37, no. 4, pp. 4575-4588, April 2022, doi: 10.1109/TPEL.2021.3121701.

[22] C. He, J. Zhu, S. Li, Z. Chen and W. Wu, "Sizing and Locating Planning of EV Centralized-Battery-Charging-Station Considering Battery Logistics System," in IEEE Transactions on Industry Applications, vol. 58, no. 4, pp. 5184-5197, July-Aug. 2022, doi: 10.1109/TIA.2022.3168244.

[23] S. Nazari, F. Borrelli and A. Stefanopoulou, "Electric Vehicles for Smart Buildings: A Survey on Applications, Energy Management Methods, and Battery Degradation," in Proceedings of the IEEE, vol. 109, no. 6, pp. 1128-1144, June 2021, doi: 10.1109/JPROC.2020.3038585.

[24] W. Gao, X. Li, M. Ma, Y. Fu, J. Jiang and C. Mi, "Case Study of an Electric Vehicle Battery Thermal Runaway and Online Internal Short-Circuit Detection," in IEEE Transactions on Power Electronics, vol. 36, no. 3, pp. 2452-2455, March 2021, doi: 10.1109/TPEL.2020.3013191.